How to Cite
Wendri, N., & Suharta, W. G. (2023). Study of magnetization of ferrite with Rare Earth and Ca substitutions. *International Journal of Chemical & Material Sciences*, *6*(1), 15-21. https://doi.org/10.21744/ijcms.v6n1.2169

Study of Magnetization of Ferrite with Rare Earth and Ca Substitutions

N Wendri
Department of Physics, Faculty of Mathematics and Natural Science, Udayana University, Denpasar, Indonesia

Wayan Gede Suharta
Department of Physics, Faculty of Mathematics and Natural Science, Udayana University, Denpasar, Indonesia
Corresponding author email: gede_suharta@unud.ac.id

Abstract*---This research synthesized nano-ferrite with Rare Earth substitution using the co-precipitation method. The main goal was to produce nanometer-sized RE/Ca-(Fe3O4) ferrite utilizing sand as the primary raw material. This research also sought to generate public interest in natural resources to maximize their benefits. Sand is abundantly available in Indonesia and is commonly used in the production of concrete, bricks, and roads. To obtain nanometer-scale particles, the co-precipitation method was employed in this study. Initially, iron sand was dissolved in HCl, stirred until homogeneous, filtered and NH4OH was added. The mixture was then precipitated, filtered and washed through a repetitive process until the nano-ferrite particles were obtained. To enhance the magnetic properties, rare earth elements (RE) were introduced during the ferrite formation. The results of FTIR characterization revealed absorbance at 1000, 1400, 1600 and 3400 cm-1, indicating vibrations caused by stretching vibrations of the metal-oxygen tetrahedral band, stretching and HOH vibrations of anti-symmetrical NO stretching vibrations arising from the nitrate group still present in the sample. XRD characterization demonstrated a spectrum predominantly composed of RE/Ca-(Fe3O4) with a purity exceeding 90%, along with the detection of SiO2 impurities. Substitution of Gd, GdNd, and Nd results in an increase in lattice constant values for the a, and b-axis, however, decrease for c-axis sequentially. Also, the substitution of Gd, GdNd, and Nd results in an increase in the coercivity and remanence magnetization values sequentially. The average particle size obtained was 150 nm.*
***Keywords*---**co-precipitation, ferrite, magnetization, x-ray diffraction.

Introduction

Research on ferrite is increasingly being carried out related to several applications including microwave devices (Thakur & Gupta, 2016), and antenna rods (Prakash et al., 2020). This study investigated the nanometer-sized RE/Ca-ferrite ferrofluid materials through the incorporation of Ca and rare earth doping using the co-precipitation method (Theiss et al., 2016). Locally available sand was employed as a natural raw material that is abundant in nature and commonly utilized in the production of concrete, bricks, and other materials in Indonesia. Interestingly, these natural materials possess significant economic potential due to their high content of iron-oxide compounds (Fe_3O_4/Fe_2O_3) in the form of iron sand, both exploited and untapped, that exist in various regions of Indonesia. This research focuses on studying sand as a natural source of iron oxide, which will undergo further processing to produce magnetic nanoparticles.

Ferrite is a magnetic material composed of iron and oxide ions, and its magnetic properties are attributed to the presence of magnetic ions known as cations. It possesses a spinel structure referred to as ferro-spinel, which is closely related to the crystal structure of spinel $MgO.Al_2O_3$ (Thakur et al., 2020).

The spinel structure consists of two types of arrangements: tetrahedral and octahedral structures. Ferro-fluid, on the other hand, is a magnetic nanomaterial in liquid form consisting of particles with dimensions of approximately 10 nm. The magnetic characteristics of ferrite can be controlled through the process of doping. In previous studies (Bueno et al., 2008; Gul et al., 2008; Peng et al., 2004), researchers have utilized divalent metals M = Mn, Co, Ni,

ISSN 2632-9468
Submitted: 09 April 2023|Revised: Date 18 2023| Accepted: 27 June 2023

Cu and Zn, in various molar ratios denoted as x in the formula M_xFe_3-xO_4, to manipulate the magnetic properties (Rafique et al., 2013; Ali, 2017). Theoretically, the magnetic strength of M_xFe_3-xO_4 can be enhanced by incorporating an Mn^{+2} cation, which has a magnetic moment per atom of 5μB, larger than that of Fe^{+2} (4μB), following the molar content (x). Conversely, the magnetic properties of ferrite magnets can be diminished by utilizing cations with lower magnetic moments such as Co^{+2} (3μB), Ni^{+2} (2μB), Cu^{+2} (1μB) and Zn^{+2} (0). In another research conducted by Mohammad Hosein Sham and colleagues, the addition of Ba (barium) doping treatment to Mg-Ti compounds was carried out to investigate the electromagnetic wave absorption characteristics (Shams et al., 2008).

The properties of the final product obtained in the production of ferrite are influenced by the methods and conditions employed. In the wet method, the necessary salts, serving as the foundation materials, are dissolved together in an acidic solvent. To achieve high homogeneity, a homogeneous solution is formed, and NaOH precipitate is added. Alternatively, NH_4OH precipitate can also be utilized, offering advantages such as the ability to remove any remaining NH_4OH contaminants in the precipitate through high-temperature heating.

Ferrite, in general, possesses a BCC (Body Centered Cubic) structure where all axes have equal lengths and the angle between them is 90º degrees. Within the ferrite family, there are various terms used to describe combinations or mixtures of iron (Fe) and carbon (C) ions. The first combination is pure ferrite, which has a structure primarily composed of Fe and contains a small amount of carbon (less than 0.01% at room temperature). It is commonly known as iron. The second combination is Austenite, which represents the Fe structure at high temperatures (above 912ºC). The third combination is Cementite, which is a mixture of iron (Fe) and iron carbide (Fe_3C). Cementite is a hard substance. The fourth combination is Pearlite, which is a mixture of ferrite and cementite. The fifth combination is Martensite, which is a combination of Fe and carbon. Martensite possesses extremely hard properties.

Several methods of ferrite have been carried out by previous researchers such as the use of co-precipitation (Zipare et al., 2015; Dubey & Kain, 2018; Arévalo et al., 2017), gamma irradiation (Zorai et al., 2023), sol-gel (Gore et al., 2017), and hydrothermal methods (Nejati & Zabihi, 2012). While variations of doping have also been carried out by several researchers such as Cr (Lakshmi et al., 2016), and Cu (Surashe et al., 2020).

The synthesis of RE/Ca-ferrite nanoparticle ferrofluid used sand as raw material through the co-precipitation method. The rare earth elements selected for this study were Yttrium (Y), Neodymium (Nd) and Gadolinium (Gd) to gain desirable magnetic properties with significant magnetic field values. The co-precipitation method was employed to generate ferrite compounds with particle sizes on the nanometer scale.

Experiment

The nano-ferrite Fe_3O_4 synthesis process involved the use of permanent magnets for extraction. HCl was added, and the mixture was stirred at 50ºC for 10 hours. The obtained results were filtered and treated with NH_4OH, followed by another round of stirring at 50ºC for 10 hours. The filtered results were then washed. Once the nano-ferrite powder Fe_3O_4 was obtained, the synthesis process for Fe_3O_4 nano-fluid was initiated. The synthesis process for RE/Ca-Fe_3O_4 nano-ferrofluid is followed:

- Weighing of the starting material Fe_3O_4, $CaCO_3$, Gd_2O_3, Nd_2O_3 based on the molar composition ratio;
- Dissolving the starting material with HCl to be mixed using a magnetic stirrer to form a homogeneous mixture;
- The homogeneous mixture was heated at a temperature of 100ºC until it thickened;
- Compounds in the form of crust were sintered at 600ºC for 2 hours;
- Surfactant was added.

To determine the success of the synthesis process, these characterizations and measurements were carried out:

- XRD (X-ray Diffraction) characterization to identify the crystallinity of the formed phase;
- SEM characterization to examine the particle size and morphology;
- FTIR characterization to analyze the functional groups of compounds formed;
- LIBS characterization to determine the elements that make up the compound.

Results

Figure 1 presents the FTIR characterization results for RE/Ca-(Fe_3O_4) samples, where RE elements (Gd, GdNd, and Nd) were varied and subjected to the calcination process at 600ºC. These figures display absorption patterns within the wave-number region, which are largely similar but differ in terms of absorption percentage.

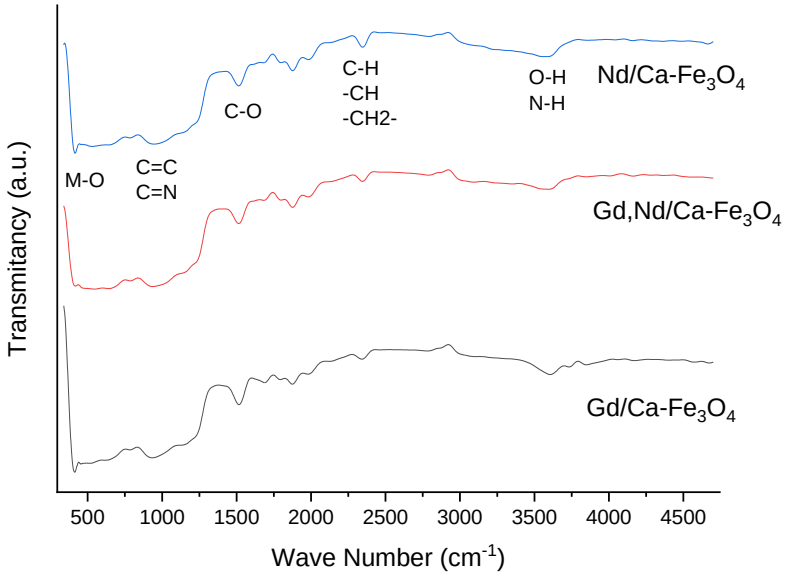

Figure 1. The FTIR characterization results for RE/Ca-(Fe_3O_4) samples

Figure 1 exhibits absorbance peaks at 1724 cm^{-1} and 1635 cm^{-1}, indicating the presence of an asymmetric carbonyl group, representing COOH and COO-, respectively. The symmetric stretching of the same carbonyl group is observed at frequencies of 1445 cm^{-1} and 1389 cm^{-1}. The range of 1665-1565 cm^{-1} encompasses the frequencies of asymmetric carbonyl stretching. Within the range of 1000-350 cm^{-1}, two broad metal-oxygen (M-O) bands are observed in the infrared spectrum, notably a ferrite-specific band at 407 cm^{-1} attributed to the stretching vibrations of the metal-oxygen tetrahedral band. The spectrum further illustrates a distinct band between 3400 and 1600 cm^{-1}, associated with the stretching and vibrational modes of H-O-H. The presence of the nitrate group is indicated by a band near 1400 cm^{-1}, resulting from anti-symmetric N-O stretching vibrations that persist in the sample.

The synthesized RE/Ca-(Fe_3O_4) sample is in the form of powder. The powdered sample was subjected to X-ray Diffraction (XRD) characterization, utilizing an angle (2θ) ranging from 10 to 90º degrees (Nath et al., 2020). Figure 2 displays the results of the XRD characterization of the RE/Ca-(Fe_3O_4) samples. Overall, the XRD spectra exhibit well-defined and smooth peaks, indicating the complete crystallization of the sample. The spectra demonstrate a consistent pattern in terms of both the position of the 2θ angle and the relative intensity of each peak. Notably, several peaks with high intensity are observed at the angles of 24.21º, 33.23º, 35.73º, 40.97º, 49.51º, 54.15º, 62.57º and 64.05º.

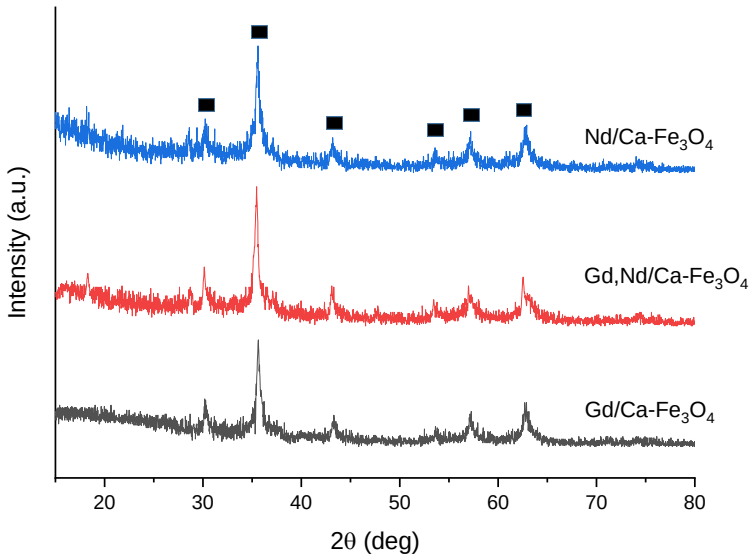

Figure 2. The XRD characterization results for RE/Ca-(Fe_3O_4) samples

The results of the X-Ray Diffraction (XRD) characterizations were analyzed using the Match! 3. Program Match! 3 aims to observe the RE/Ca-(Fe_3O_4) phase and the impurity phase in the sample by referring to the reference database in the form of a PDF (powder Diffraction File) contained in the program. However, several peaks do not match with the reference peaks, indicating the presence of impurity phases. These non-matching peaks are referred to as impurity phases. By referring to the appropriate reference, namely PDF number 00-033-0664, the sample can be identified as a compound of Iron Oxide Fe_3O_4 (hematite). Furthermore, the impurity phase corresponds to PDF number 00-046-1045, which is silicon oxide SiO_2 (quartz). The calculated volume fractions for each sample are presented in Table 1. The inclusion of RE doping elements (Y, Nd, Gd and Eu) results in volume fraction values exceeding 90%, with variations among the different samples.

Table 1
The calculation volume fractions for RE/Ca-(Fe_3O_4) samples

No	Sample	Volume fraction (%)
1	Gd/Ca-(Fe_3O_4)	92.1
2	Gd, Nd/Ca-(Fe_3O_4)	91.8
3	Nd/Ca-($Fe3O_4$)	90.6

The Volume Fraction percentages for each sample are reported in Table 1, with Gd/Ca-(Fe_3O_4) at 92.1 %, GdNd/Ca-(Fe_3O_4) at 91.8 %, and the sample Nd/Ca-(Fe_3O_4) at 90.6 %. These results indicate a successful synthesis process, although the volume fraction does not reach 100 %. Additional sintering processes can be conducted to remove the impurity phase or achieve a volume fraction of 100 %, but this would require extra time and cost. Nevertheless, with a volume fraction exceeding 90%, the samples can still be applied effectively (Adnyana & Suarbawa, 2022).

To assess the suitability of the obtained spectra in this study with reference, a Rietveld analysis was performed using the Rietica software. This program also calculates lattice constant values, density, unit cell volume and particle size. The results of the Rietveld analysis for the RE/Ca-(Fe_3O_4) sample demonstrate lattice parameter values in the a-axis direction, b-axis direction, and c-axis direction.

The refinement results of the ferrite samples are presented in Table 2, showcasing varied lattice constant values. For the Gd/Ca-(Fe_3O_4) sample, the lattice constants along the a-axis, b-axis and c-axis are 5.954745(4), 5.887364(2) and 16.873253(5) Å, respectively. Regarding the GdNd/Ca-(Fe_3O_4) sample, the lattice constants along the a-axis, b-axis and c-axis are 6.129565(4), 5.934412(6) and 16.808916(8), respectively. Lastly, the Nd/Ca-(Fe_3O_4) sample exhibits lattice constants along the a-axis, b-axis and c-axis are 6.245926(3), 5.973536 (5) and 16.769247(4), respectively.

Table 2
The refinement results for RE/Ca-(Fe_3O_4) samples (lattice constants along the a-axis, b-axis and c-axis

No	Sample	Lattice constants along the a-axis (Å)	Lattice constants along the b-axis (Å)	Lattice constants along the c-axis (Å)
1	Gd/Ca-(Fe_3O_4)	5.954745(4)	5.887364(2)	16.873253(5)
2	Gd, Nd/Ca-(Fe_3O_4)	6.129565(4)	5.934412(6)	16.808916(8)
3	Nd/Ca-(Fe_2O_4)	6.245926(3)	5.973536 (5)	16.769247(4)

In this study, the sample densities for Gd/Ca (Fe_3O_4), GdNd/Ca-(Fe_3O_4), and Nd/Ca-(Fe_3O_4) were 9.682 gr/cm^2, 9.784 gr/cm^2, and 9.685 gr/cm^2, respectively and the average particle size obtained from the result is 150 nm.

VSM Characterization Results

VSM characterization results of the samples are shown in Figures 3a to 3c. The value of coercivity (Ec), remanence magnetization (Dr) and saturation magnetization (Ds) of the samples are shown in Table 3. Coercivity values of RE/Ca-(Fe_3O_4) are increased by 0.002, 0.004, and 0.040 kOe, with the substitution of Gd, GdNd and Nd elements, respectively. The remanence magnetization values were 0.001x10^{-2}, 0.002x10^{-2}, and 0.100x10^{-2} emu/g, for the addition of Gd, GdNd and Nd, respectively. Meanwhile, the saturation magnetization values were 14.00x10^{-2}, 2.90x10^{-2}, and 1.55x10^{-2} emu/g, respectively of Y, Gd and Nd substitution. The data shows an increase in coercivity and remanence magnetization values with Y, Gd and Nd element substitutions respectively (Yu et al., 2000).

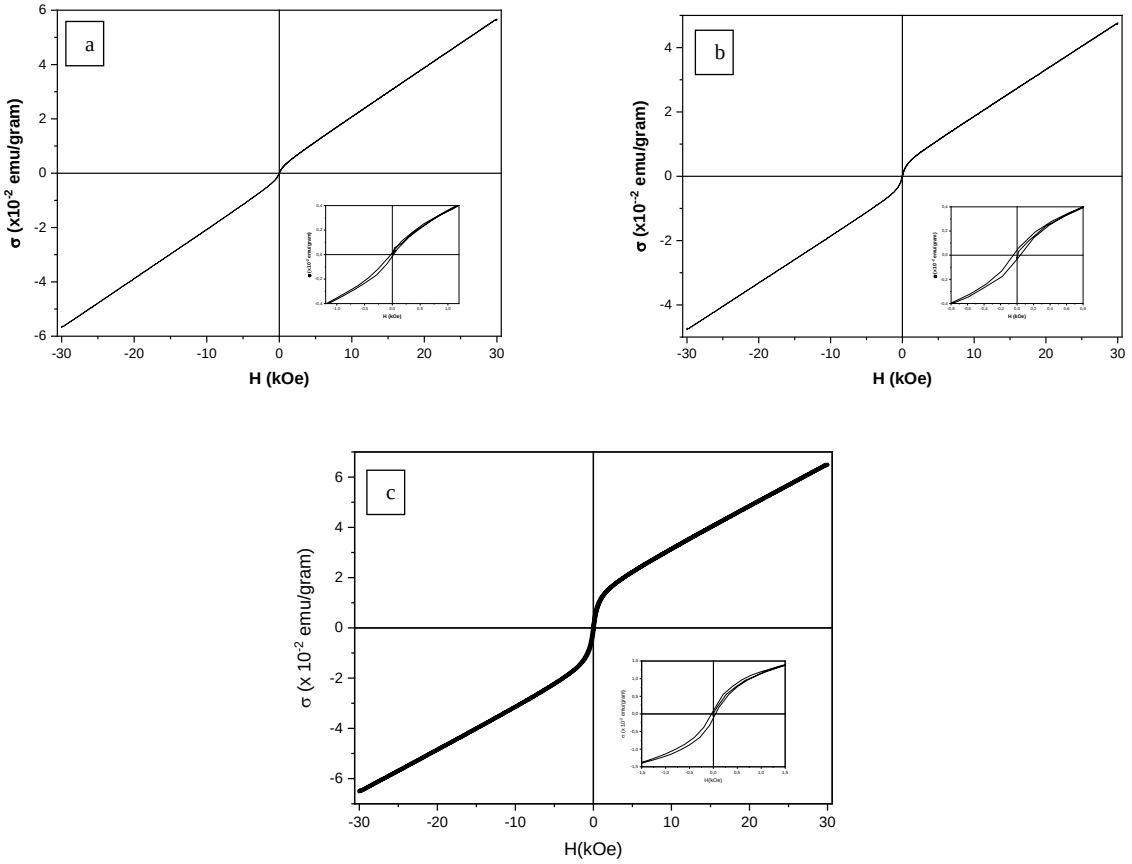

Figure 3. The VSM characterization results for RE/Ca-(Fe_3O_4) samples: a) Gd/Ca (Fe_3O_4); b) GdNd/Ca-(Fe_3O_4); c) Nd/Ca-(Fe_3O_4)

Table 3
The value of Ec, Dr and Ds of all samples

Sample	Ec (kOe)	Dr (emu/g)	Ds (emu/g)
Gd/Ca (Fe_3O_4)	0.002	0.001 x 10^{-2}	0.320 x 10^{-2}
GdNd/Ca (Fe_3O_4)	0.004	0.002 x 10^{-2}	0.260 x 10^{-2}
Nd/Ca (Fe_3O_4)	0.040	0.100 x 10^{-2}	0.400 x 10^{-2}

Conclusion

Based on the synthesis, characterization, and analysis conducted in this study using the Match and Rietica software, several conclusions can be drawn as follows:

- The successful synthesis of RE/Ca-(Fe_3O_4) samples in powder form with high purity, indicated by volume fractions exceeding 90 % (ranging from 90.6 % and 92.1 %).
- Substitution of Gd, GdNd, and Nd results in an increase in lattice constant values for the a, and b-axis, however, decrease for c-axis sequentially.
- Substitution of Gd, GdNd, and Nd results in an increase in the coercivity and remanence magnetization values sequentially.

References

Adnyana, I. G. A. P., & Suarbawa, K. N. (2022). Study of the effect of lanthanum and cerium doping combination on magnetic properties of M-type hexaferrite oxide permanent magnets. *International Journal of Chemical & Material Sciences*, *5*(1), 34-37. https://doi.org/10.21744/ijcms.v5n1.2052

Ali, R. (2017). *The Impacts of Various Metal Cations on Structural, Dielectric and Magnetic Properties of Nanocrystalline Nickel and Magnesium Ferrites* (Doctoral dissertation, The Islamia University of Bahawalpur).

Arévalo, P., Isasi, J., Caballero, A. C., Marco, J. F., & Martín-Hernández, F. (2017). Magnetic and structural studies of Fe3O4 nanoparticles synthesized via coprecipitation and dispersed in different surfactants. *Ceramics International*, *43*(13), 10333-10340. https://doi.org/10.1016/j.ceramint.2017.05.064

Bueno, A. R., Gregori, M. L., & Nobrega, M. C. (2008). Microwave-absorbing properties of Ni0. 50–xZn0. 50–xMe2xFe2O4 (Me= Cu, Mn, Mg) ferrite–wax composite in X-band frequencies. *Journal of Magnetism and Magnetic Materials*, *320*(6), 864-870. https://doi.org/10.1016/j.jmmm.2007.09.020

Dubey, V., & Kain, V. (2018). Synthesis of magnetite by coprecipitation and sintering and its characterization. *Materials and Manufacturing Processes*, *33*(8), 835-839.

Gore, S. K., Jadhav, S. S., Jadhav, V. V., Patange, S. M., Naushad, M., Mane, R. S., & Kim, K. H. (2017). The structural and magnetic properties of dual phase cobalt ferrite. *Scientific reports*, *7*(1), 2524.

Gul, I. H., Ahmed, W., & Maqsood, A. (2008). Electrical and magnetic characterization of nanocrystalline Ni–Zn ferrite synthesis by co-precipitation route. *Journal of magnetism and magnetic materials*, *320*(3-4), 270-275. https://doi.org/10.1016/j.jmmm.2007.05.032

Lakshmi, M., Kumar, K. V., & Thyagarajan, K. (2016). Structural and magnetic properties of Cr-Co nanoferrite particles. *Advances in nanoparticles*, *5*(01), 103-113.

Nath, D., Singh, F., & Das, R. (2020). X-ray diffraction analysis by Williamson-Hall, Halder-Wagner and size-strain plot methods of CdSe nanoparticles-a comparative study. *Materials Chemistry and Physics*, *239*, 122021. https://doi.org/10.1016/j.matchemphys.2019.122021

Nejati, K., & Zabihi, R. (2012). Preparation and magnetic properties of nano size nickel ferrite particles using hydrothermal method. *Chemistry Central Journal*, *6*, 1-6.

Peng, C. H., Wang, H. W., Kan, S. W., Shen, M. Z., Wei, Y. M., & Chen, S. Y. (2004). Microwave absorbing materials using Ag–NiZn ferrite core–shell nanopowders as fillers. *Journal of magnetism and magnetic materials*, *284*, 113-119. https://doi.org/10.1016/j.jmmm.2004.06.026

Prakash, J., Khan, S., Chauhan, S., & Biradar, A. M. (2020). Metal oxide-nanoparticles and liquid crystal composites: A review of recent progress. *Journal of Molecular Liquids*, *297*, 112052. https://doi.org/10.1016/j.molliq.2019.112052

Rafique, M. Y., Pan, L. Q., Iqbal, M. Z., Qiu, H. M., Farooq, M. H., Guo, Z. G., & Tanveer, M. (2013). Growth of monodisperse nanospheres of MnFe2O4 with enhanced magnetic and optical properties. *Chinese Physics B*, *22*(10), 107101.

Shams, M. H., Salehi, S. M. A., & Ghasemi, A. (2008). Electromagnetic wave absorption characteristics of Mg–Ti substituted Ba-hexaferrite. *Materials Letters*, *62*(10-11), 1731-1733. https://doi.org/10.1016/j.matlet.2007.09.073

Surashe, V. K., Mahale, V., Keche, A. P., Alange, R. C., Aghav, P. S., & Dorik, R. G. (2020). Structural and electrical properties of copper ferrite (CuFe2O4) NPs. In *Journal of Physics: Conference Series* (Vol. 1644, No. 1, p. 012025). IOP Publishing.

Thakur, P., Chahar, D., Taneja, S., Bhalla, N., & Thakur, A. (2020). A review on MnZn ferrites: Synthesis, characterization and applications. *Ceramics international*, *46*(10), 15740-15763. https://doi.org/10.1016/j.ceramint.2020.03.287

Thakur, V. K., & Gupta, R. K. (2016). Recent Progress on Ferroelectric Polymer-Based Nanocomposites for High Energy Density Capacitors: Synthesis, Dielectric Properties, and Future Aspects. *Chemical reviews*, *116*(7), 4260-4317.

Theiss, F. L., Ayoko, G. A., & Frost, R. L. (2016). Synthesis of layered double hydroxides containing Mg2+, Zn2+, Ca2+ and Al3+ layer cations by co-precipitation methods—A review. *Applied Surface Science*, *383*, 200-213. https://doi.org/10.1016/j.apsusc.2016.04.150

Yu, L. Q., Zheng, L. J., & Yang, J. X. (2000). Study of preparation and properties on magnetization and stability for ferromagnetic fluids. *Materials Chemistry and Physics*, *66*(1), 6-9. https://doi.org/10.1016/S0254-0584(00)00236-4

Zipare, K., Dhumal, J., Bandgar, S., Mathe, V., & Shahane, G. (2015). Superparamagnetic manganese ferrite nanoparticles: synthesis and magnetic properties. *J. Nanosci. Nanoeng*, *1*(3), 178-182.

Zorai, A., Souici, A., Dragoe, D., Rivière, E., Ouhenia, S., Belloni, J., & Mostafavi, M. (2023). Superparamagnetic cobalt ferrite nanoparticles synthesized by gamma irradiation. *New Journal of Chemistry*, *47*(5), 2626-2634.